Geomechanics and Engineering, *Vol. 31, No. 5 (2022) 489-503*
https://doi.org/10.12989/gae.2022.31.5.489

Measured structural response of a long irregular pit constructed using a top-down method

Yang Sun*[1], Yufei Che[1], Zhenxue Gu[2], Ruicai Wang[1] and Yawen Fan[3]

[1]*College of Harbour, Coastal and Offshore Engineering, Hohai University, No. 1 Xikang Road, Nanjing, Jiangsu, P.R. China*
[2]*Shanghai Shen Yuan Geotechnical Engineering Co., Ltd, No. 1368 Tibet South Road, Shanghai, P.R. China*
[3]*College of Telecommunications and Information Engineering, Nanjing University of Posts and Telecommunications, No. 66 New Model Road, Nanjing, Jiangsu, P.R. China*

(*Received May 30, 2020, Revised November 13, 2022, Accepted November 23, 2022*)

Abstract. A 1257-m-long irregular deep foundation pit located in the central of Nanjing, China was constructed using the combined full-width and half-width top-down method. Based on the long-term field monitoring data, this study analyzed the evolution characteristics of the vertical movement of the columns, internal force of the struts, and axial force of the structural beam and slab. The relevance of the three mentioned above and their relationship with the excavation process, structural system, and geological conditions were also investigated. The results showed that the column uplift was within the range of 0.08% to 0.22% of the excavation depth, and the embedded depth ratio of the diaphragm wall and the bottom heave affected significantly on the column uplift. The differential settlement between the column and diaphragm wall remained unchanged after the base slab was cast. The final settlement of the diaphragm wall was twice the column uplift. The internal force of the struts did not varied monotonically but was related to numerous factors such as the excavation depth, number of struts, and environmental conditions. Additionally, the dynamic force and deformation of the columns, beams, and slabs were analyzed to investigate the inherent relationship and variation patterns of the responses of different parts of the structure.

Keywords: field monitoring; internal force variation; internal structure; irregular foundation pit; top-down method

1. Introduction

With the development of urban construction, urban underground spaces such as subway stations and underground shopping malls have been gradually developed and utilized, increasing the area and depth of foundation pit excavations. The combined support system with inner columns and struts has been widely used as an economical and effective support method (Kim *et al.* 2016, Zhang *et al.* 2018b). Deep foundation pit projects are generally located in urban areas with dense facilities such as existing buildings, roads, and underground pipelines and are influenced by a myriad of factors. Moreover, the stress and deformation of the structure dynamically change with the progress of construction (Elbaz *et al.* 2016, Kon 2017, Ding *et al.* 2017, Hu and Ma 2018). It is very difficult to conduct an accurate stress and deformation analysis, and hence field monitoring must be carried out. Due to the technical characteristics of the top-down construction method, the monitoring of the vertical movement of the columns as well as the internal forces of the strut structure and beam-slab structure has become one of the main aspects of such project field monitoring. By analyzing the monitoring data, the forces on the support structure can be determined in a timely manner and its deformation roughly inferred to ensure the stability of the pit and the surrounding buildings.

With the development of large-scale and complex foundation pit projects, the requirements on the computational theory (Peck 1969, Celep and Güler 1991, Paik and Salgado 2003, Yang 2007), numerical analysis (Ng 1992, Han 2014, Li *et al.* 2015, Ukritchon *et al.* 2016, Zheng *et al.* 2017a, Zhang *et al.* 2018a, Jiang *et al.* 2018), and field monitoring for foundation pit excavation and support are also increasing (Bolton *et al.* 2014, Liu *et al.* 2015, Chambers *et al.* 2016, Zhang *et al.* 2016). In terms of field monitoring, Boone and Crawford (2000), and Wu *et al.* (2019) proposed that the temperature increment can affect the variation of the strut load. Lin (2011) conducted a shrinkage-induced pull-out test on a 264-m-long reinforced concrete (RC) strut; the monitoring data showed that the shrinkage of the ultralong RC struts can generate tension on the strut structure; dividing the extra-long concrete into short sections and densely placing vertical support columns helped to control the tensile stresses and the expansion of wall deflection, and the effect of strut shrinkage and corresponding control measures were proposed. Liu *et al.* (2011) used the monitoring data of similar deep foundation pits in Shanghai, Singapore, and Taiwan to study the difference between the settlements of the columns and the diaphragm walls. The results showed that the maximum uplifts of the columns and the diaphragm wall were 30 and 16 mm, respectively. The measured ratio of the column uplift to the pit excavation depth was less than 0.1%, while the observed ratio of the diaphragm wall uplift to the excavation depth was approximately 0.04%. Tan and Li

*Corresponding author, Associate Professor
E-mail: sunyang_hhu@hhu.edu.cn

ISSN: 2005-307X (Print), 2092-6219 (Online)

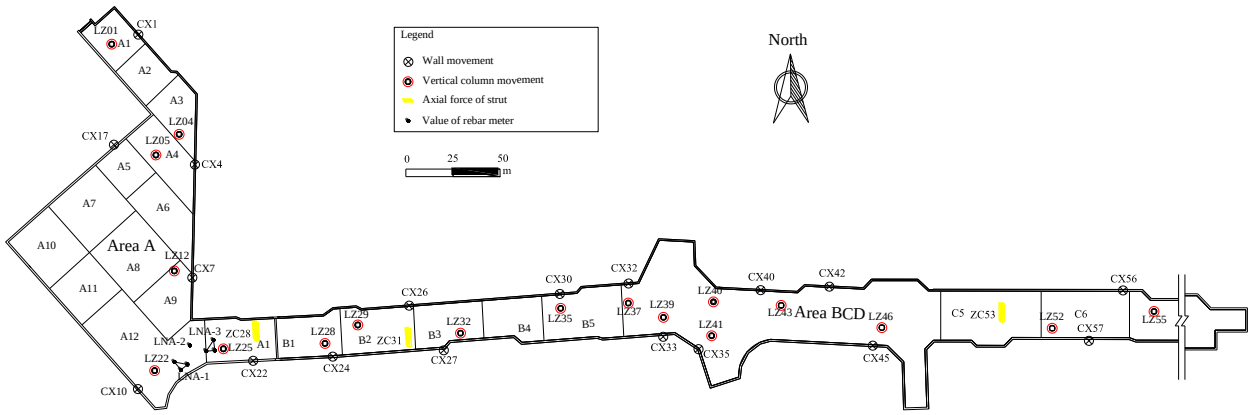

Fig. 1 Layout of excavation and instrumentation

(2011) examined the field monitoring data of a 26-m deep foundation pit excavation project constructed using the top-down method in the urban area of Shanghai and found that the average column uplift was approximately 0.06% of the excavation depth and that the column uplift and the maximum lateral displacement of the diaphragm wall showed a linear relationship with a ratio of 0.6 between the two. The concrete strut slab and the joint beam and slab strut withstood the system load due to soil unloading, and their axial forces were related to the soil pressure behind the diaphragm wall. Goh *et al*. (2017) investigated the forces on struts of propped excavations in clay by 2D and 3D finite element analysis and found that the difference in support force for different L/B (2Dvs3D) depends on the clay type, L/B ratio and support level. Numerical analysis and field monitoring were conducted to investigate the performance of retaining system with different combinations of long-short columns by Xu *et al.* (2020). Results showed that the number and length of the column affected the bottom heave and the movement of column. Thus a reliable and economical structural bracing system could be designed by optimizing the number and length of columns.

To date, research on the stress and deformation characteristics of the internal structure of a foundation pit continues progress. However, the columns, struts, and horizontal beam-slab form an interactive three-dimensional structure, in which their internal forces and deformation interact with each other. The complexity of the top-down method makes such three-dimensional characteristic features more prominent. Therefore, it is necessary to conduct a comprehensive analysis based on a combination of a variety of relevant factors to fully understand the evolution patterns and thus perform a reasonable prediction of the future development trend of the foundation pit. In this study, based on the long-term field monitoring data of a 1257-m-long irregular deep foundation pit project in Nanjing, China, the evolution characteristics of the movement of columns, internal force of the struts, and internal force of the beam and slab structure were analyzed, and the correlation among the three mentioned above as well as their relationship with the excavation process, structural system, and geological conditions were investigated.

2. Project overview

The Hunan Road underground commercial street project is located in the central area of Nanjing. It is an ultralong irregular foundation pit constructed using the full-width and half-width top-down method and a complex excavation process and structural system. The accurate analysis of the stress and deformation of the internal structure during the foundation pit construction process is critical to ensuring the stability of the support structure and the foundation pit as a whole. In this study, the stress and deformation (mainly including the vertical movement of the columns, axial force of the horizontal beam-slab, and internal force of the struts) of the internal structure of the foundation pit were analyzed based on the field monitoring data of this project.

Due to the need for traffic coordination and rerouting on the roads above the foundation pit, a mixed full-width and half-width top-down construction method was employed in the project. A plan view of the project is shown in Fig. 1. This project consisted of two parts, namely, the Shanxi Road sunken plaza (Area A) and the Hunan Road underground commercial street (Areas B, C, and D). The foundation pit has a total length of 1257 m. Area A is a three-level basement, and Areas B, C, and D are two-level basements. According to environmental protection requirements and changes in load conditions, diaphragm walls with thicknesses of 0.8 m and 1.0 mm, respectively, were selected for the vertical enclosure. The “beam-slab structure + temporary struts” were used as horizontal strut members. In Area A, concrete struts were used, and in Areas B, C, and D, steel struts were used for the first level and concrete struts for the other two levels. Each column of the foundation pit included a steel pipe pile with a diameter of 0.6 m placed on top of an engineering pile with a diameter of 1.0 m. To ensure the resumption of traffic on Hunan Road as early as possible, parts of Areas C and D were changed from full-width to half-width construction, and the strut mode was adjusted to a three-level RC strut slab structure.

The top-down construction method is used to excavate the foundation pit level by level from the roof slab down.

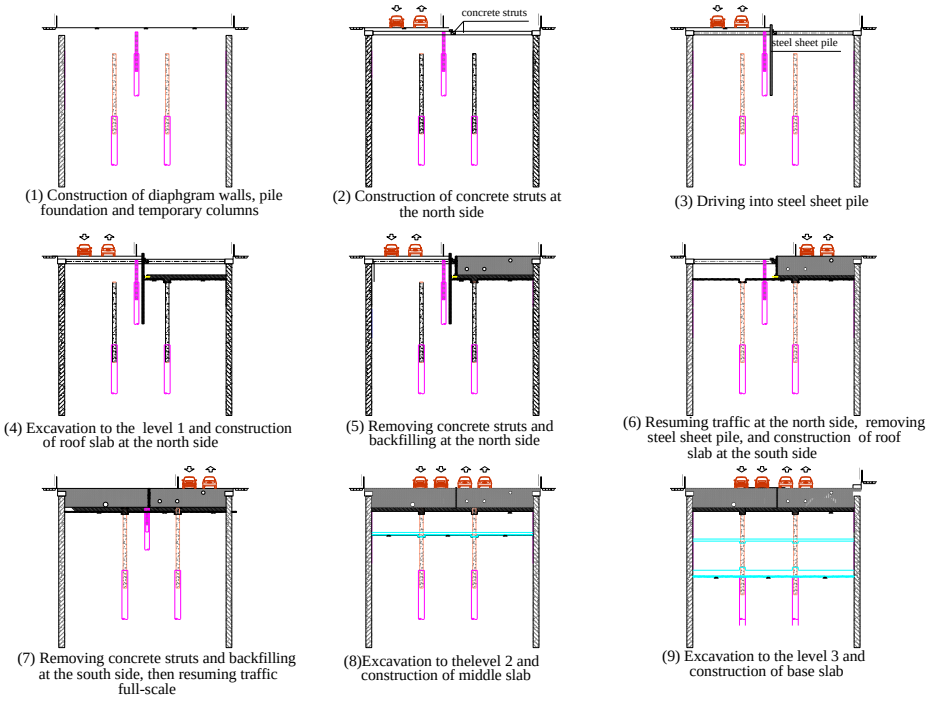

Fig. 2 Semi-construction sequence in Areas C and D

Table 1 Construction stages of block A13 in Area A

Stage	Event	Date	Days spent
1	Construction of diaphragm walls and pile foundation	2015.1.14 ~ 2016.5.25	498
2(a)	Excavation surface soil at elevation of 7.8 m	2016.5.26 ~ 2016.6.25	29
2(b)	Construction of roof slab (B0F) at elevation of 10.3 m	2016.6.26 ~ 2016.7.24	29
2(c)	Casting of roof slab	2016.7.25 ~ 2016.8.7	14
2(d)	Backfilling and resuming traffic	2016.8.7 ~ 2016.10.18	73
3(a)	Excavation to the elevation of 2.6 m	2016.10.18 ~ 2016.11.8	22
3(b)	Dewatering construction	2016.12.2 ~ 2016.12.22	21
3(c)	Construction of middle slab 1 (B1F) at elevation of 4.1 m	2016.12.23 ~ 2017.1.18	27
3(d)	Casting of middle slab 1	2017.1.19 ~ 2017.4.6	88
4(a)	Excavation to the elevation of -1.4 m	2017.4.6 ~ 2017.5.28	53
4(b)	Construction of middle slab 2 (B2F) at elevation of 0.1 m	2017.7.7 ~ 2017.9.21	77
4(c)	Casting of middle slab 2	2017.9.22 ~ 2017.11.6	66
5(a)	Excavation to the elevation of -7.4 m	2017.11.6 ~ 2017.11.20	15
5(b)	Construction of base slab at elevation of -4.9 m	2017.11.20 ~ 2018.1.1	15
5(c)	Casting of base slab	2018.1.1 ~ 2018. 1.29	28

The construction method is divided into full-width and half-width construction. Fig. 2 shows the construction process of the half-width construction in Areas C and D. This method divides the part above the roof slab into two halves, and the construction stages below the roof slab are the same as those in the top-down method. This project were excavated at the same time. The construction began on January 20, 2015. Tables 1-3 summarize the detailed construction procedures of typical construction blocks in Areas A, B, and C, respectively. The construction method in Area D is

Table 2 Construction stages of block B2 in Area B

Stage	Event	Date	Days spent
1	Construction of diaphragm walls and pile foundation	2015.11.9 ~ 2016.5.30	204
2(a)	Excavation of surface soil to elevation of 7.1 m	2016.5.24 ~ 2016.5.30	6
2(b)	Installation of steel pipe struts (Ø609) at elevation of 10.5 m	2016.5.25 ~ 2016.5.30	6
2(c)	Construction of roof slab (B0F) at elevation of 9.1 m	2016.6.1 ~ 2016.6.25	25
2(d)	Casting of roof slab	2016.6.26 ~ 2016.7.18	23
2(e)	Removing steel pipe struts	2016.7.18 ~ 2016.7.19	2
2(f)	Backfilling and resuming traffic	2016.8.5 ~ 2016.8.8	3
3(a)	Excavation to the elevation of 2.0 m	2016.10. ~ 2016.10.23	16
3(b)	Dewatering construction	2016.11. ~ 2016.11.24	24
3(c)	Construction of middle slab (B1F) at elevation of 4.0 m	2016.12.1 ~ 2017.1.8	38
3(d)	Casting of middle slab	2017.1.8 ~ 2017.3.4	56
4(a)	Excavation to the elevation of -4.0 m	2017.3.4 ~ 2017.3.18	15
4(b)	Construction of base slab at elevation of -1.5 m	2017.4.18 ~ 2017.7.3	77
4(c)	Casting of base slab	2017.7.3 ~ 2017.7.31	28

Table 3 Construction stages of block C6 in Area C

Stage	Event	Date	Days spent
1	Construction of diaphragm walls, pile foundation and temporary columns	2016.1.1 ~ 2016.8.8	221
2	Dewatering construction at the north side	2016.8.16 ~ 2016.8.17	2
3	Backfilling and resuming traffic at the south side	2016.8.25 ~ 2016.9.2	9
4	Construction of concrete struts at the north side	2016.9.17 ~ 2016.9.30	14
5	Driving into steel sheet pile	2016.10.1 ~ 2016.10.10	10
6(a)	Excavation to the elevation of 6.5 m at the north side (level 1)	2016.10.9 ~ 2016.11.1	24
6(b)	Construction of roof slab (B0F) at elevation of 8.2 m at the north side	2016.11.2 ~ 2016.11.24	23
6(c)	Casting of roof slab at the north side	2016.11.25 ~ 2016.12.1	6
7(a)	Removing concrete struts at the north side	2016.12.1	1
7(b)	Backfilling and resuming traffic at the north side	2016.12.5 ~ 2017.1.13	39
8	Dewatering construction at the south side	2017.1.14 ~ 2017.1.15	2
9	Removal of steel sheet	2017.1.16 ~ 2017.1.17	2
10(a)	Excavation to the elevation of 6.5 m at the south side (level 1)	2017.1.18 ~ 2017.1.23	6
10(b)	Construction of roof slab (B0F) at elevation of 8.2 m at the south side	2017.2.6 ~ 2017.2.22	17
10(c)	Casting of roof slab at the south side	2017.2.23 ~ 2017.3.3	8
11(a)	Removing concrete struts at the south side	2017.3.4	1
11(b)	Backfilling at the south side and resuming traffic full-scale	2017.3.4 ~ 2017.4.19	47
12(a)	Excavation to the elevation of 1.1 m	2017.4.20 ~ 2017.5.30	41
12(b)	Construction of middle slab (B1F) at elevation of 3.1 m (level 2)	2017.6.19 ~ 2017.8.6	49
12(c)	Casting of middle slab	2017.8.7 ~ 2017.9.10	35
13(a)	Excavation to the elevation of -4.7 m	2017.9.10 ~ 2017.11.28	79
13(b)	Construction of base slab (B1F) at elevation of -2.2 m (level 3)	2017.12.6 ~ 2018.1.11	36
13(c)	Casting of base slab	2018.1.12 ~ 2018.2.9	28

similar to that in Area C and is not repeated herein. The sectional diagram of the support structure is shown in Fig. 3.

According to the results of the in situ soil tests (standard penetration test, dynamic penetration test, borehole wave velocity test, and permeability test) and laboratory tests

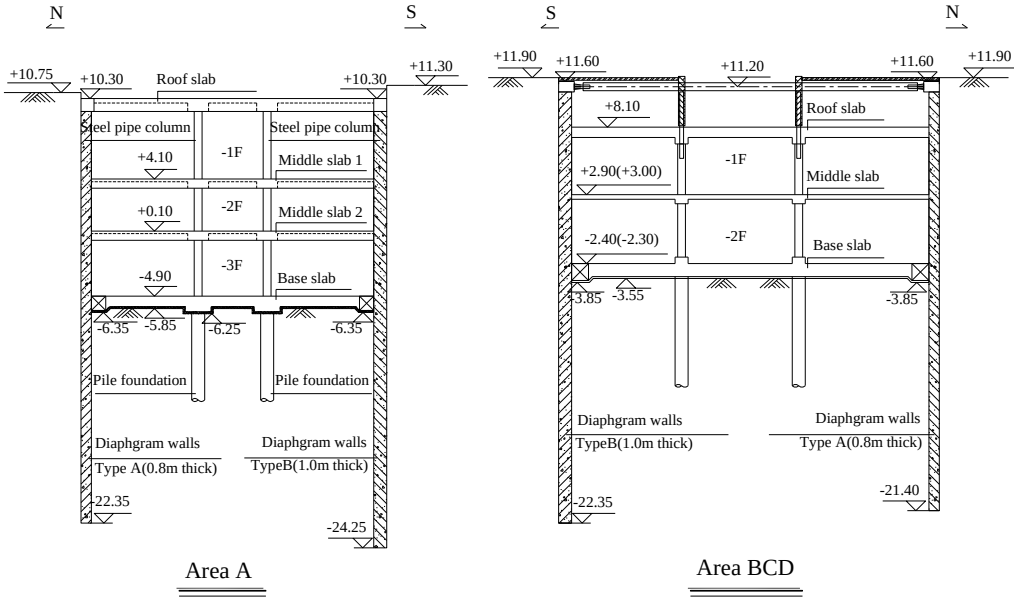

Fig. 3 Cross section of the excavation support structure

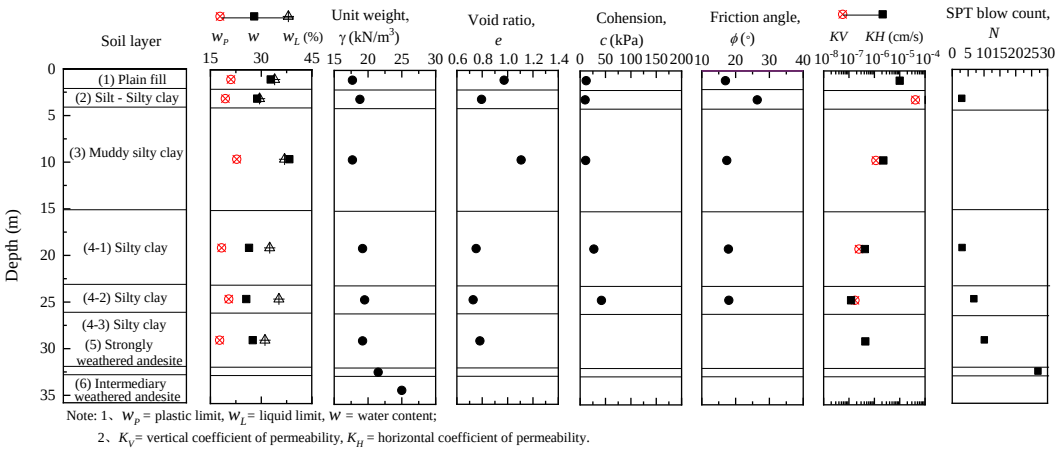

Fig. 4 Soil profiles and part of soil parameters

(shear box test and triaxial test) data, the soil profiles and soil properties are shown in Fig. 4. The groundwater level exhibited seasonal variation. During the survey, the underground water level measured by the survey was 1.20~2.20 m, and the stable water level was 0.70~1.75 m.

3. Layout of measuring points

Fig. 1 shows the planar layout of the monitoring and measuring points for the foundation pit of the project. The focus of this study is to monitor the vertical movement of the columns, slab internal force of the support structure, and beam axial force of the strut structure.

3.1 Monitoring of vertical movement of columns

According to the design requirement, the number of measuring points was 20% of the total number of columns. Among them, there were 142 piles of a “one column with one pile” type in Area A, there were 265 piles of a “one column with one pile” type in Areas B, C, and D, and the number of piles with monitoring points was not less than 82. The vertical movement of the columns (marked as LZ1-LZ83) in this project was monitored by electronic levels.

3.2 Monitoring of the internal force of the support slab structure

A total of 21 locations were selected in Areas A, B, C and D. Among them, 9 monitoring points were selected for the internal force of the slab structure in Area A, and 4 rebar stress gauges were deployed at each monitoring point for internal force monitoring, amounting to a total of 36 rebar stress gauges in Area A. In Areas B, C, and D, 12 monitoring points were selected for the internal force of the slab structure, and 4 rebar stress gauges were deployed at each monitoring point for internal force monitoring,

amounting to a total of 48 rebar stress gauges in this area to monitor the magnitude and variation of the internal force of the support structure with the excavation of the foundation pit and the progress of the basement construction.

3.3 Monitoring of the axial force of the structural beam strut

To grasp in a timely manner the various working stages of the earth excavation and underground construction of the foundation pit and the stress on the strut as well as its variation and development, a beam was selected at each of the three levels at the border between Area A and Area B, amounting to 3 beams for the three levels; the axial stress was measured using the rebar stress gauge. A beam was selected at a typical location of the second underground level in Area B, and the axial stress was measured using the rebar stress gauge. Four rebar strain gauges were deployed at each monitoring cross section, and a total of 16 rebar stress gauges were installed to monitor the magnitude and variation of the strut axial force with the excavation of the foundation pit and the progress of the underground project construction.

4. Monitoring results and analysis

4.1 Column vertical movement

4.1.1 Development trend of vertical column movement

There are many factors affecting the vertical movement of the columns, including the strut system of the foundation pit, the column self-weight, the properties of the soil strata, the pit bottom rebound, and the upper load. Among them, the pit bottom rebound and the loads on top of the column play a dominant role. Fig. 5 shows the curves of the vertical movement with time for selected representative columns in Areas A, B, and C. In Fig. 5, the vertical axis L_h denotes the vertical movement value of a column, with positive and negative values representing settlement and uplift, respectively. As shown in Fig. 5, when the foundation pit was excavated, the stress at the bottom of the pit was released, and the soil inside the pit rebounded and deformed; the pile shaft was subjected to an upward frictional resistance and hence was uplifted. When the earth was excavated at the first basement level, regardless of whether the column was in Area A, B, or C, the column did not exhibit any vertical movement. This phenomenon may be because the depth of excavation at the first basement level was small, and hence the pit bottom rebound is small. Under this situation, the column had a large insertion depth and its lateral frictional resistance was large, hindering the uplift of the column. In addition, a three-dimensional structure, which consisted of the enclosure structure, horizontal struts, and column, jointly withstood the load, resulting in a good overall stability and less susceptibility of the column to uplift. When the earth was excavated at the minus two and minus three levels, column uplift occurred.

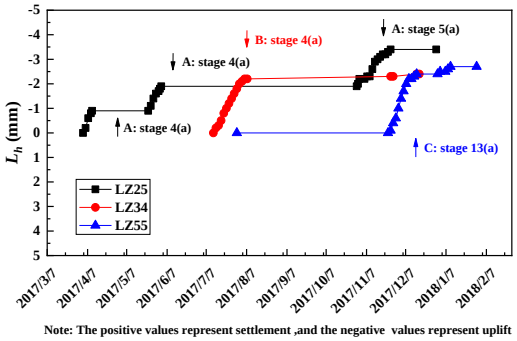

Fig. 5 Development of vertical column movements during excavation

Based on the assumption that there is no column uplift when the earth was excavated at the first basement level of the pit, theoretically column LZ25 in Area A would undergo a total of two times of uplift, one occurring when the earth was excavated at the second level and the other at the third level. However, two times of column uplift occurred when the earth was excavated at the minus two level. This may be because column LZ25 is located at the edge of Area A13 and was affected by the excavation of earth at the minus two level in Area A12. When the earth was excavated at the minus two level, the uplift values of the columns in Areas A, B and C, were roughly comparable; when the earth was excavated at the minus three level, the columns underwent another round of uplift. Overall, the uplift height of the columns in Area A was slightly larger than that of the columns in Areas B and C. After excavation, the columns basically did not undergo vertical movement. During the entire foundation pit construction process, the columns basically did not undergo settlement and, overall, column uplift occurred. Compared with the initial stage when the foundation pit was not yet excavated, the column was in an uplift state. This indicates that the slab pile load and the column self-weight cannot offset the effect of the rebound of the bottom of the excavated soil on the vertical movement of the column. The long-term uplift of the column should be continuously monitored after the completion of the construction. In general, the uplift values of the columns in this project were no more than 4mm. Since a good strut system was established in the project, the construction could be carried out by levels and blocks in an orderly manner, and proper construction methods could help to limit the column settlement.

4.1.2 Relationship between column settlement and excavation depth

Fig. 6 shows the relationship between the column uplift and the excavation depth and shows that the columns in this project mainly exhibited a state of uplift, which was in the range of 1 to 4 mm. Overall, the column uplift was in the range of 0.08% H to 0.22% H. Specifically, the column uplift in Area A was in the range of 0.13% H to 0.22% H, the column uplift in Area B was in the range of 0.08% H to 0.22% H, and the column uplift in Area C was in the range of 0.15% H to 0.22% H. Due to differences in various factors such as the foundation pit shape, strut system, and

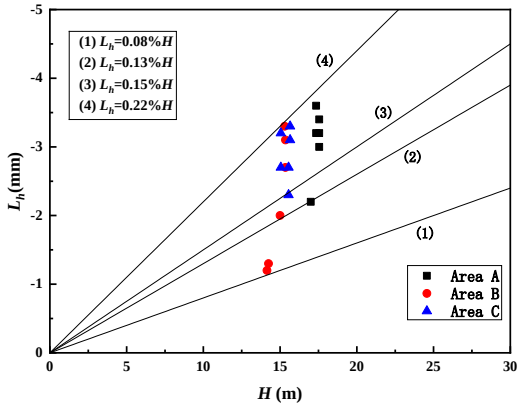

Fig. 6 Relationships between L_h and H

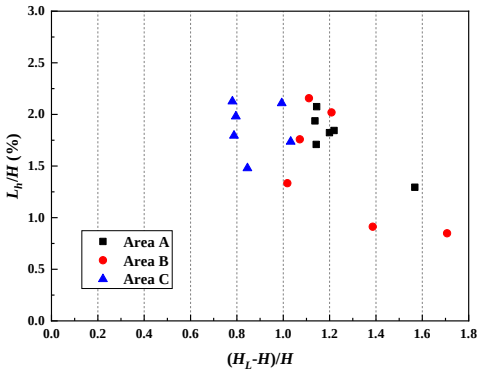

Fig. 7 Effect of the embedded depth ratio of the column on vertical movements

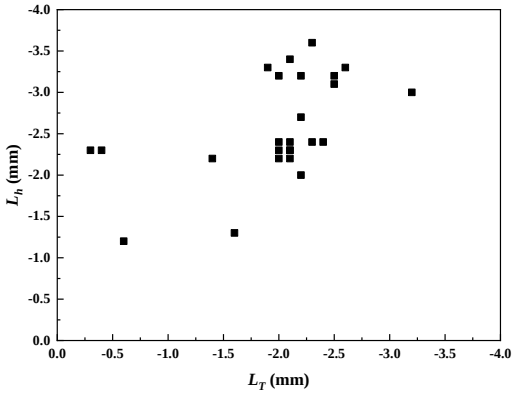

Fig. 8 Relationship between L_h and L_T

construction method among Areas A, B and C, there are differences in the ratio of the column uplift to the excavation depth of the foundation pit in the three areas, but the difference is small. For columns in different areas, as the depth of the foundation pit excavation increased, the column uplift tended to increase. However, overall, the difference in the column uplift under the different excavation depths was not significant, indicating that when the other conditions remained the same, the column uplift increased with the excavation depth. In addition, in addition to the excavation depth, there may be other factors affecting the vertical movement of the column, requiring further investigation.

4.1.3 Effect of column embedded depth ratio on vertical column movement

Fig. 7 shows the effect of the column embedded depth ratio on the vertical movement of a column, where L_h is the final vertical movement value of the column, H is the excavation depth of the foundation pit, H_L is the length of the column, and $(H_L$-$H)/H$ is defined as the column embedded depth ratio. As shown in Fig. 7, the embedded depth ratio of the columns in this project was concentrated in the range of 0.8 to 1.7. As an overall trend, with the increase in the embedded depth ratio, the dimensionless vertical movement value of the column decreased. This indicates that when the column embedded depth ratio increased, the side frictional resistance of the column increased, which can effectively hinder the vertical movement. However, more monitoring data are needed to support the investigation of whether this hindrance effect will be strengthened with the increase in the embedded depth ratio and whether it will not be further strengthened after a certain embedded depth ratio is reached.

4.1.4 Effect of pit bottom rebound vertical column movement

Fig. 8 demonstrates the relationship between the vertical movement of the column and the rebound of the bottom of the pit. It can be seen from Fig.8 that the vertical movement of the column is approximately linearly related to the pit bottom rebound, that is, the larger the tip bottom rebound, the larger the column uplift. However, the increase of the column uplift is lower than that of the pit bottom rebound, indicating that the compression of the column by the upper load, horizontal strut system, and pile shaft friction all effectively suppressed the column uplift. In addition, even when the tip bottom rebound did not occur, the column had already undergone the uplift, indicating that after the excavation of the foundation pit, the column uplift occurred prior to the pit bottom rebound. Therefore, priority should be given to suppressing the column uplift.

4.1.5 Relationship between the vertical movement of the column and the maximum lateral displacement of the enclosure structure

By establishing the relationship between the uplift of the column and the lateral displacement of the enclosure structure, the monitored lateral displacement of the enclosure structure can be used to predict the vertical movement tendency of the column. Fig. 9 demonstrates the relationship between the vertical movement of the columns and the maximum lateral displacement of the enclosure structure. It can be seen from Fig. 9 that the columns were all uplifted, and the uplift value was stable and in the range of 1 mm to 4 mm, which was not significantly related to the lateral displacement of the enclosure structure. This indicates that there could be other factors affecting the vertical movement of the columns, and further analysis is needed.

Due to the large stress-strain field caused by the settlements of the columns and the diaphragm wall, the superstructure and foundation base are at risk of damage.

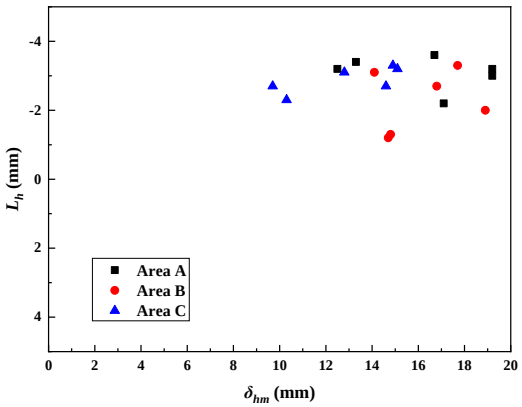

Fig. 9 Relationships between L h and δ hm

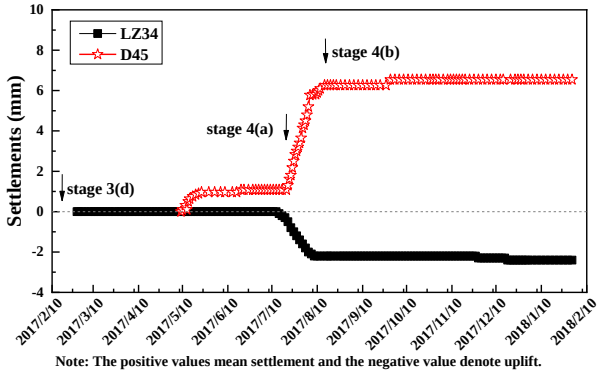

Fig. 10 Development of vertical column movements and diaphragm wallsettlements during excavation

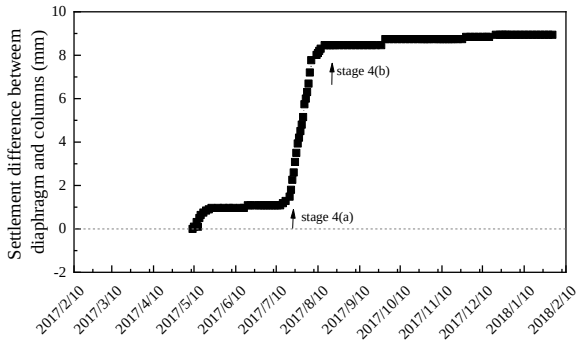

Fig. 11 Development of the difference between vertical column movements and diaphragm wall settlements during excavation

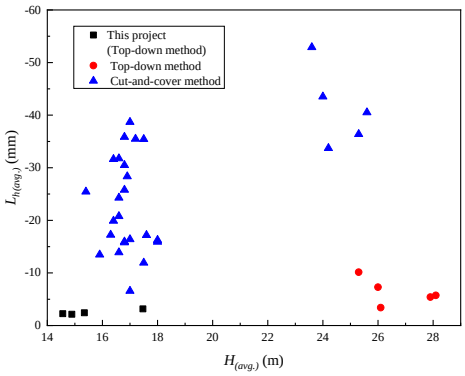

Fig. 12 Relationships between vertical column movements and excavation methods

Therefore, it is necessary to study the evolution trend of the differential settlement between the columns and the diaphragm wall. Fig. 10 shows the curves of the vertical movements of the column and the adjacent diaphragm wall with time, where a positive value means settlement and a negative value denotes uplift, and Fig. 11 shows the curves of the settlement difference between the diaphragm wall and the column. It can be seen from the figures that when the earth at the minus two level was excavated, the column and the adjacent diaphragm wall underwent large vertical movements, the column was uplifted, and the diaphragm wall settled. In addition, as the excavation process progressed, the variations of the two increased, and the settlement difference between the diaphragm wall and the column also increased. After the base slab was cast, neither the column nor the diaphragm wall exhibited significant vertical movement, and the settlement difference remained at a stable value. Before the excavation of the earth at the minus two level, a small settlement occurred at the top of the diaphragm wall. Based on the construction conditions, measuring point D45 was located near the border between Areas B4 and B5. Approximately on May 10, 2017, the earth in the minus two level of Area B5 began to be excavated, affecting the adjacent diaphragm wall and resulting in the settlement of the diaphragm wall in the vicinity of measuring point D45, when there was no uplift of the column. In addition, after the base slab was constructed, the final settlement value of the diaphragm wall was approximately twice the final uplift value of the column. These phenomena indicate that in the construction process, the settlement of the diaphragm wall was more affected by the foundation pit excavation, which should be given due attention during the construction process.

4.1.6 Relationship between vertical column movement and excavation methods

Fig. 12 shows the relationship between the vertical column movements under two excavation methods, namely, the top-down method and cut-and-cover method, and the excavation depth. In Fig. 12, the horizontal axis is the average excavation depth, and the vertical axis is the average uplift value of the column. In addition to the data from the measuring points in this study, the rest of data were from the foundation pit of the Tianjin subway station as studied by Zheng(2017b). It can be seen from Fig. 12 that the uplift of the column under the top-down method is stabilized within 10 mm, and the uplift of the column under the cut-and-cover method is between 5 mm and 55 mm, which is far greater than that under the top-down method. This is because, under the top-down method, the slab and horizontal strut at each level form a highly rigid space structure with the enclosure structure and columns to jointly withstand the loads and effectively limit the uplift of the columns; at the same time, the slab at each level exerts a downward load on the column to counteract the column rebound caused by the earth excavation and pit bottom

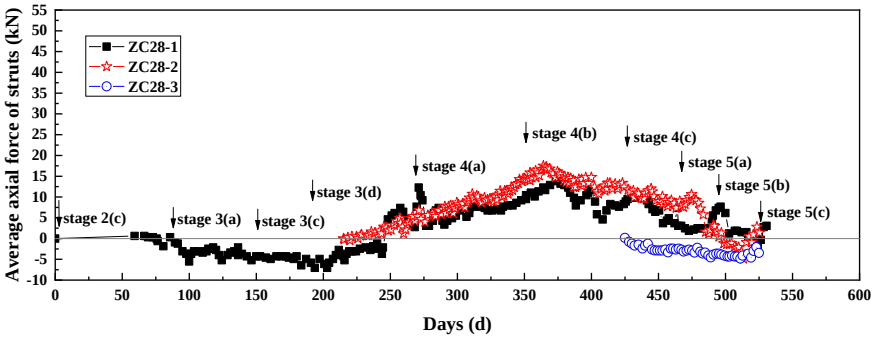

Note: The positive values indicate that the concrete beam is in compression and the negative values indicate that the concrete beamin tension, respectively.

(a) Development of axial force of struts in Area A

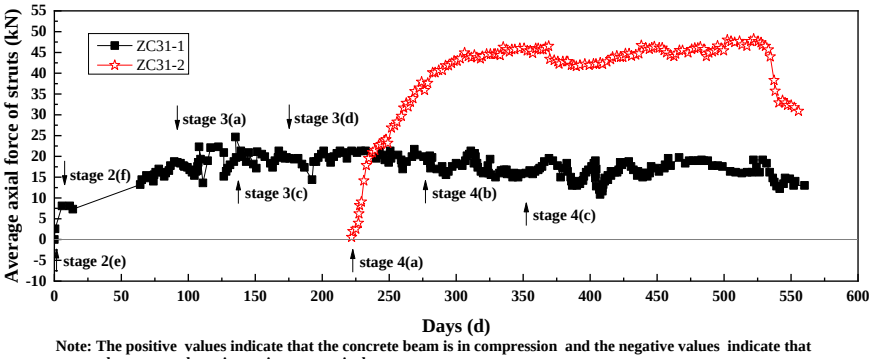

Note: The positive values indicate that the concrete beam is in compression and the negative values indicate that the concrete beamin tension, respectively.

(b) Development of axial force of struts in Area B

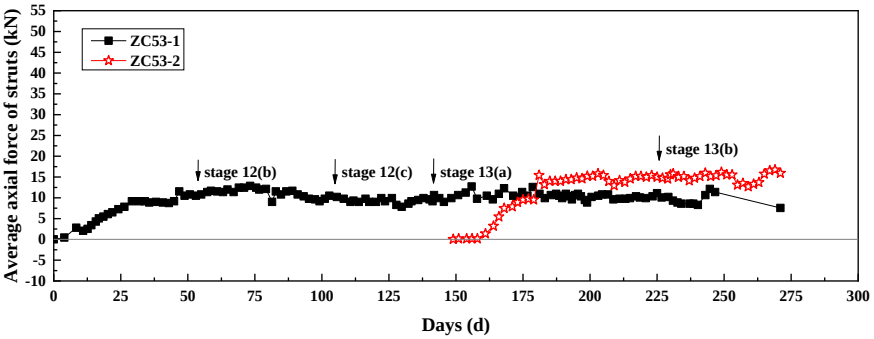

Note: The positive values indicate that the concrete beam is in compression and the negative values indicate that the concrete beamin tension, respectively.

(c) Development of axial force of struts in Area C

Fig. 13 Development of axial force of struts in different areas of excavation

rebound, thus decreasing the amount of uplift. Combined with the data of other foundation pits, it was found that the column uplift exhibited an increasing trend as the excavation depth of the foundation pit increased, regardless of use of the top-down method or the cut-and-cover method.

4.2 Internal forces of struts

Since the top-down method was used in the construction of the foundation pit of this project, structural beams were also used as horizontal strut members for the foundation pit. Fig. 13 shows a diagram of the internal force variation of the structural beam in each area of the pit. The vertical axis represents the axial force of the structural beam, with positive and negative values indicating that the concrete beam is in compression and in tension, respectively. Typical structural beams in Areas A, B, and C were selected for the analysis. It can be seen from Fig. 13(a) that the axial forces were generated in beams at various levels of Area A in the late phase of the curing stage and the actual axial forces were far lower than the design values (7500 kN for Beam B0, 5300 kN for Beam B1, and 5300 kN for Beam B2). When earth was excavated at the first basement level, Beam B0 (i.e., roof beam) was in tension, and the axial force increased as the excavation depth increased. When Beam B1 was being constructed and cured, the axial force of Beam B0 stabilized at a roughly fixed value. During the concrete curing process of Beam B1, its stress state gradually changed from tension to compression. As the excavation depth at the minus two level increased, the axial force of Beam B1 increased rapidly. At this time, Beam B0 was in compression, and the axial force also increased with

the excavation depth. At this stage, Beam B0 and Beam B1 jointly withstood the active earth pressure of the soil behind the wall after the earth excavation. With the construction of Beam B2, the axial force of Beam B0 and Beam B1 tended to decrease. After the construction of Beam B2 was completed and it was cured, it gradually entered tension. When the burden level was being excavated and the base slab was being constructed, the axial forces of Beam B0 and Beam B1 continued to decrease, and that of Beam B2 increased slightly and stabilized at a fixed value. After the construction of the base slab was completed, the axial forces of the beams at each level tended to stabilize and varied slightly in the range of -5 kN to 5 kN. As time elapsed, the concrete beam shrank to some extent, and at this time, the structural beam was subjected to tensile stress. When the beam needed to bear the earth pressure on the outside of the foundation pit, the beam gradually changed from compression to tension. When Beam B0 and Beam B1 could resist the earth pressure on the outside of the foundation pit, Beam B2 bore less earth pressure. At this time, the stress of Beam B2 was mainly determined by the drying shrinkage deformation of the beam itself. It can be seen from Fig. 13 that the development of the axial force of each slab beam did not increase or decrease monotonically but changed constantly with the progress of the foundation pit construction and was closely related to the deformation of the foundation pit. When the excavation depth was small, the top of the diaphragm wall moved toward the outside of the pit, and the strut beam was in tension; when the excavation depth was large, the diaphragm wall moved to the inner side of the pit, and the strut beam was squeezed at the two ends of the beam, causing the stress state to change to compression. The weather has a considerable effect on concrete strut beams; high temperature, rain, and snow can affect the deformation of concrete itself, thus resulting in changes to the beam axial force. For example, from day 300 to day 400 after the initial measurement, that is, from June to September of 2017, when the weather was hot and the temperature was high, the concrete struts might undergo heat-induced elongation, causing the lateral displacement of the surrounding diaphragm wall. The interaction between the beam and the support structure made both Beam B0 and Beam B1 subjected to compression at this time, and the peak compression occurred at this stage. When constructing slab B2, the axial forces of Beam B0 and Beam B1 in Area A reached their maximum values, while the axial force of Beam B2 did not show a significant peak value. In addition, the construction of the base slab had little impact on the axial force variation of the beams at each level. After the construction of the base slab, the axial forces of the beams at each level all basically fluctuated within a stable range. Because the axial force variation of the beam-slab after the completion of the construction was not monitored, it was not possible to describe the long-term axial force variation of the structural beam.

It can be seen from Fig. 13(b) that the axial force of Beam B0 in Area B increased significantly after the steel struts were removed, and the rate of increase was extremely fast. When the overburden soil at the top was backfilled, the axial force of Beam B0 continued to increase due to the increased upper load. When excavating the earth at the first basement level as well as all subsequent construction behaviors, the axial force of Beam B0 fluctuated approximately 20 kN, showing no significant trend of increasing or decreasing. For Beam B1, the first monitoring was carried out when the earth was excavated at the minus two level. With the increase of the excavation depth and the construction of the base slab, the axial force of Beam B1 increased significantly, and the magnitude of the axial force was significantly larger than that of Beam B0, indicating that the earth pressure at the minus two level was mainly taken by Beam B1. After the base slab was constructed, the axial force of Beam B1 stabilized at a fixed value. Approximately 520 days after the initial measurement of Beam B0, the axial forces of Beam B0 and Beam B1 both decreased. This was estimated to be in January, when the climate was cold. This result may be jointly driven by factors including soil creep as well as the shrinkage-induced deformation of concrete.

It can be seen from Fig. 13(c) that when excavating the earth at the next level, the axial forces of both Beam B0 and Beam B1 in Area C increased significantly in a linear fashion. Before the construction of the slab beam at the lower level, the axial force of the slab beam at the upper level reached the maximum value. After that, the axial force of the slab beam at the upper level did not change significantly and stabilized at a roughly fixed value. In addition, when excavating the earth at the minus two level, the axial force of Beam B0 slightly decreased, indicating that Beam B1 played the main role in bearing the earth pressure at the minus two level where the earth was excavated and shared the pressure on Beam B0.

Combining Figs. 13(a)-13(c), the general development pattern of the axial force of the slab beams in the foundation pit can be summarized as follows:

(1) The axial force of the beam at each level of the foundation pit was generally generated when the earth was excavated at the lower level or slightly preceding the excavation of the earth at the lower level. The axial force developed significantly and tended to increase linearly with time, reaching its maximum value when the slab beam at the lower level was being constructed.

(2) Under normal conditions, the foundation pit beam was in compression; however, under special circumstances (e.g., when the diaphragm wall moved outward and the concrete shrank in the initial stage of the excavation), the concrete slab beam was in tension.

(3) As various construction items progressed, the axial force of the beams at each level did not increase or decrease monotonically but rather followed a complex process that was related to a variety of factors including the excavation depth, number of struts, concrete properties, upper load, soil characteristics, and ambient conditions.

Fig. 14 shows a diagram of the axial force variation of the temporary struts in Areas B and C of the foundation pit. The horizontal axis represents the time when the initial measurement of the erected struts was completed, and the vertical axis represents the axial forces of the temporary struts, with positive and negative values denoting compression and tension, respectively. The steel struts were erected in Area B,

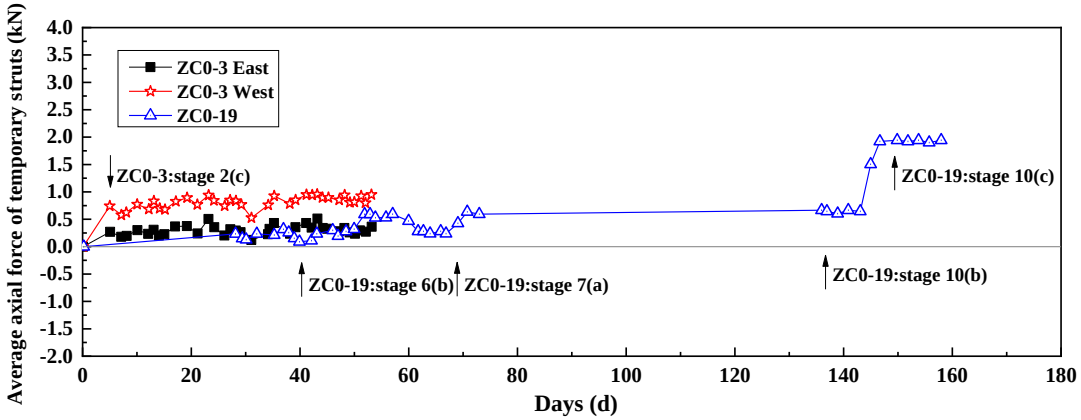

Note: The positive and negative values denote compression and tension, respectively.

Fig. 14 Development of axial force of temporary struts in Areas B & C

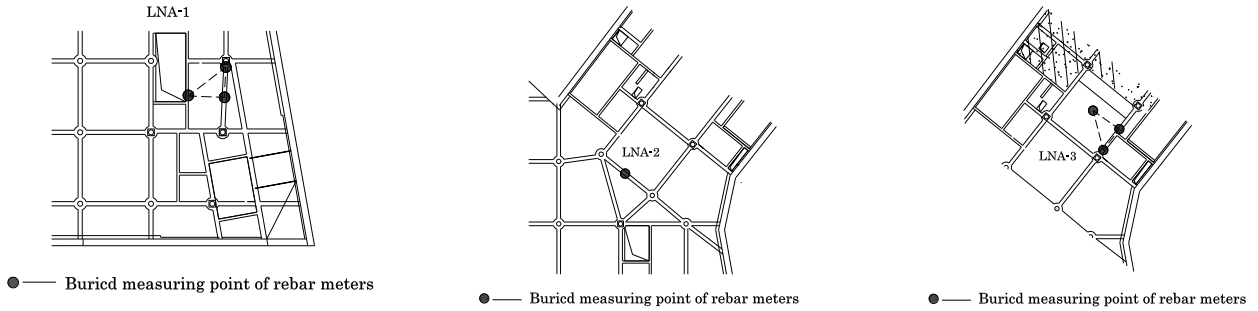

(a) The first basement in Area A (b) The second basement in rea A (c) The third basement in Area A

Fig. 15 Buried measuring points of rebar meters

and concrete struts were erected in Area C. It can be seen from Fig. 14 that after the erection of the steel struts in Area B, they were in compression, and their axial forces increased immediately. At this time, the soil behind the diaphragm wall moved toward the interior of the foundation pit, and the diaphragm wall also had lateral displacement, causing the steel struts to be in compression with an increased axial force. During the period from the erection completion to the removal of the steel struts, their axial forces always fluctuated approximately 750 kN. This is because the axial force of the steel struts was also affected by various factors such as construction, temperature, and upper load. The variation of the axial force of concrete struts in Area C was more complicated than that of the steel struts in Area B. Because the half-width method was adopted for the construction of Area C, the time for the erection of the concrete struts was longer. During the construction of the northern half-width, the axial force of the struts increased slowly. During the construction of the roof slab of the northern half-width, the axial force of the struts slightly increased because at this time, the concrete struts were needed to gradually bear the earth pressure at the first basement level during the excavation of the northern half-width. After the roof slab was constructed, because the roof slab could also play a bracing role, the axial force of the concrete struts at the first level began to reduce. After the concrete struts of the northern half-width were removed, the axial force of the struts increased and remained unchanged for a long period of time. During the construction of the roof slab of the southern half-width, the axial force of the struts increased rapidly because at this time, the struts are needed to bear the earth pressure outside the entire foundation pit. After the construction of roof slab was completed, the axial force of the struts reached the maximum value and remained unchanged. Due to the different construction methods, the variation trends of the axial forces of the steel struts and concrete struts were quite different, but eventually the axial force of the steel struts was lower than that of the concrete struts. However, in this project, the axial forces of the two forms of struts were both very small, far below the design value of the axial force of the struts. In addition, it is known from the earlier discussion that there is not much difference between the two forms of struts in limiting the deformation of the top of the diaphragm wall. Therefore, the form of the struts should be properly selected to meet the needs of an actual project.

4.3 Beam-slab stress

In the process of measuring the axial force of the beam and slab, considering the symmetry of beam members under general conditions, rebar meters were tied to the upper and lower parts of the midspan of the beam and other rebar meters were welded to the upper and lower parts of the support at one end. In addition, at the center of the adjacent slabs, rebar meters were also welded in two orthogonal directions to the rebars at the top and bottom of the slab. The locations of some of the actual embedded rebar meters are shown in Fig. 15. The magnitudes of the axial forces at different locations of the same beam were analyzed to understand the dynamic changes of

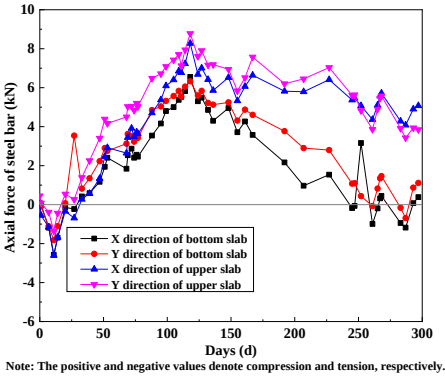

(a) Stress situation of slab

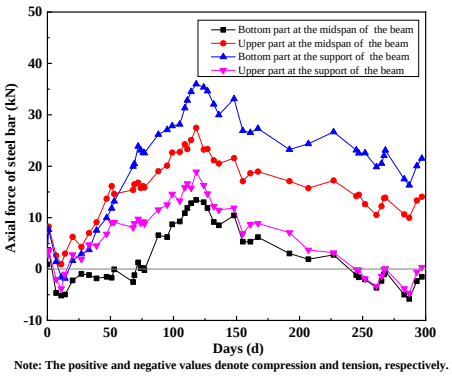

(b) Stress situation of beam

Fig. 16 Development of stress situations of slab and beam on the first basement in Area A

the structure itself during the construction, determine the spatial and temporal state characteristics of the stresses of the underground structure under various load and external force conditions, and identify the intrinsic relation and variation patterns of the response of different parts of the structure during the construction.

(1) First basement level in Area A

Fig. 16 shows the axial forces of the beam-slab at the first-level basement in Area A. The horizontal axis represents the time. After the completion of the beam and slab rebar tying, the initial monitoring was performed, and the time was recorded as day 0. After the concrete was cast and reached a certain strength, the first measurement was carried out, and the time was recorded as day 1. The vertical axis represents the force on the beam and slab, with a positive value being compression and a negative value being tension.

It can be seen from Fig. 16 that the force on the rebars in Area A had a significant time effect, and the overall trend was in a "V" shape, reaching the peak compression at around day 120, and the overall trend unexpectedly fluctuated slightly.

The first stage was from the beginning to approximately day 20, during which the construction of the beam and slab was completed, and the concrete was just cast. Because the concrete slowly started to form during this process, it had a certain strength, and the tensile stress was the largest. This is because during the initial stage, the rebars were bonded to the concrete during the forming, and hence tension was generated under this action. This stage was short but with a large slope of the curve.

The second stage was from day 20 to day 130. In this stage, the beam and the slab had already been formed and began to bear part of the load in the structure. At this time, the construction of the main structure at the second underground level continued. During the process of excavation and construction at the second underground level, the load on the structural members continued to increase, and so did the compression in the members. This stage was long but with a small slope of the curve. For example, at day 110, the excavation had reached the design elevation of Slab B2 in Area A7 and Area A10. The earth was being excavated at the minus three level in Area A4. Because the excavation was near the

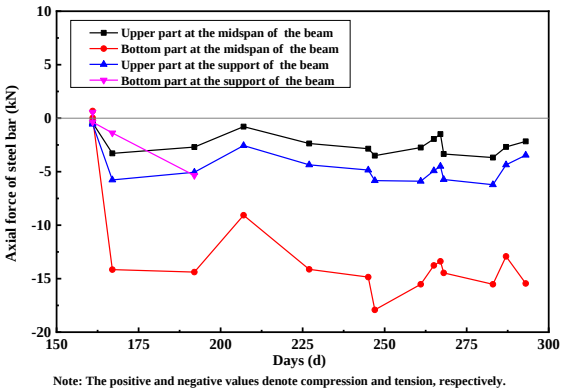

Fig. 17 Development of stress situation of beam on the second basement in Area A

base, part of the load originally borne by the underground soil was transferred to the monitoring location, resulting in a continuous increase in compression at this time.

The third stage was after day 120. During this stage, the compression in the structural members began to decrease and the curve started to rise. This is because at this time, the construction of the main structure at the second underground level was basically completed, and the excavation at the third underground level started, causing a disturbance at the second underground level, and so the curve rose. For example, at this moment, Slab B1 had already been cast, and Slab B2 in Areas A8, A9, and A11 had also been cast. As the beam and slab structure surrounding the monitoring location gradually formed, the structure at the second underground level tended to stabilize, and the compression at the monitoring location gradually decreased.

(2) Second basement level in Area A

Fig. 17 shows the axial forces of the beams at the second basement level in Area A. The horizontal axis represents the time. The initial measurement date after the completion of the rebar tying in the beam and slab at the first basement level in Area A was recorded as day 0, the initial monitoring after the completion of the rebar tying at the second basement level corresponded to day 161, and the first monitoring after the concrete casting corresponded to day 192. In this part, only the monitoring of the beam was carried out, and the corresponding slab members were not monitored.

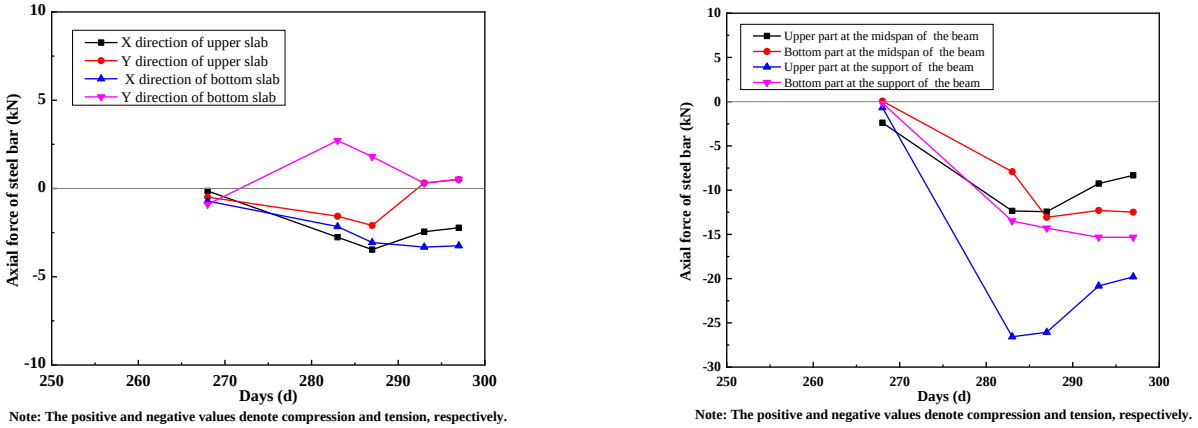

(a) Stress situation of slab (b) Stress situation of beam

Fig. 18 Development of stress situations of slab and beam on the third basement in Area A

After the beam and slab structure at the second basement level in Area A was formed, it directly bore the load of the diaphragm wall on the two sides as well as the gravity load from the upper first basement level. The internal rebars were subjected to tension. On day 207, the load decreased, and slab B0 had already been cast. Slab B1 in Areas B1-B5 had been completed, as had the base slabs in Areas B1-B4. The earth in Area A6 had been excavated to the design elevation of the base slab, and part of the base slab had been cast. The earth at the minus three level in Areas A7 and A12 was being excavated, the design elevation of the base slab had been reached locally, and the loads and forces fluctuated with the forming of adjacent structures and the excavation of the structure.

(3) Third basement level in Area A

Fig. 18 shows the axial force of the beam-slab at the third basement level in Area A. The initial measurement after the completion of the rebar tying at the third basement level in Area A corresponded to day 268, and the first measurement after the concrete casting corresponded to day 283.

The tying of the rebar meters at the third basement level in Area A was completed around December 20, 2017, and the concrete casting and curing was completed around the end of December 2017. During the measurement process, it was found that the forces in the slab varied less than 3 kN The excavation as well as the concrete casting and curing in this area had been completed, and the disturbance of the construction activities to the forces of the slabs in this area was very small. The force on the structural slab was mainly the force caused by the squeezing of the diaphragm wall on both sides and the adjacent slabs and was exerted gradually on the concrete during the process of its gradual hardening.

At this time, the main reinforcement of the beam was noticeably subjected to the tension force after the completion of the concrete casting and curing, and the tension force on the rebar in the upper parts of the beam midspan and one end of the support exhibited a gradually decreasing trend, while the force of the rebar in the lower parts of the beam midspan and one end of the support tended to increase slightly. This occurred at the third basement level in Area A, and there is no corresponding basement level in Area B. In addition, during the monitoring, Areas A1-A12 had also been cast, and the structure at this location was constructed as the last task since all of the construction in the surrounding locations had been completed and there was no more excavation work. When the structure at the monitoring location was formed, it directly bore the load of the underground structure as well as the load of the adjacent retaining wall, resulting in tensile deformation.

5. Conclusions

(1) The vertical movement of the columns was closely related to the construction conditions. In this project, the uplift of the columns was very small, all within 4 mm. The well-designed strut system, orderly construction by levels and blocks, and reasonable construction methods all helped to limit the column settlement.

(2) The uplift of columns monitored in this project was in the range of 0.08% to 0.22% *H*. When the other conditions remained unchanged, the uplift of the column increased with the excavation depth.

(3) The embedded depth ratio of the diaphragm wall and the rebound of the pit bottom had greater impacts on the uplift of the column than the lateral displacement of the diaphragm wall. The columns had improved resistance to the uplift of the excavated foundation pit than the diaphragm wall.

(4) In the construction process of this project, the column was uplifted, and the diaphragm wall settled. With the progress of the excavation process, the differential settlement between the two also increased. After the base slab was cast, the settlement difference was also maintained at a stable value, and the final settlement of the diaphragm wall was approximately twice the final uplift of the column. The vertical movement of the diaphragm wall was more susceptible to foundation pit excavation, which should be considered during the construction process.

(5) The internal force of each layer's struts of the underground structure generally arose when excavating the

next layer of earthwork or slightly before excavating the next layer of earthwork, and developed significantly. At this time, the internal force increased linearly with time. The internal force reached a maximum value during the construction of the next layer of slab. The struts were generally subjected to compression, but in special cases such as concrete shrinkage they appeared to be under tension. The internal force of the struts did not increase or decrease monotonically but was related to a variety of factors such as the excavation depth, number of struts, concrete properties, upper load, and external environmental conditions.

(6) The internal force of the temporary steel strut was less than that of the temporary reinforced concrete strut, and the reinforced concrete struts played a greater role in this project. However, both of them are much smaller than the design value of the strut internal force.

Acknowledgments

Sincere gratitude is extended to China Ershisiju Civil Engineering Group Co., Ltd. for the assistance in the field data collection. The research work described herein was funded by the National Natural Science Foundation of China (NSFC, Grant Number: 41672257) and by the Natural science foundation of Jiangsu province (Project Number: BK20160908). Their financial support is gratefully acknowledged.

References

Bolton, M.D., Lam, S.Y., Vardanega, P.J., Ng, C.W.W. and Ma, X.F. (2014), "Ground movements due to deep excavations in Shanghai: design charts", *Front. Struct. Civ. Eng*., **8**(3), 201-236. https://doi.org/10.1007/s11709-014-0253-y.

Boone, S.J. and Crawford, A.M. (2000), "Braced excavations: temperature, elastic modulus, and strut loads", *J. Geotech. Geoenviron. Eng.*, **126**(10), 870-881. https://doi.org/10.1061/(asce)1090-0241(2000)126:10(870).

Celep, Z. and Güler, K. (1991), "Dynamic response of a column with foundation uplift", *J. Sound Vib.*, **149**(2), 285-296. https://doi.org/10.1016/0022-460X(91)90637-Y.

Chambers, P., Augarde, C., Reed, S. and Dobbins, A. (2016), "Temporary propping at Crossrail Paddington station", *Geotech. Res.*, **3**, 3-16. https://doi.org/10.1680/jgere.15.00009.

Ding, Z., Wei, X.J. and Wei, G. (2017), "Prediction methods on tunnel-excavation induced surface settlement around adjacent building", *Geomech. Eng.*, **12**(2), 185-195. http://doi-org/10.12989/gae.2017.12.2.185.

Elbaz, K., Shen, S.L., Arulrajah, A., and Horpibulsuk, S. (2016), "Geohazards induced by anthropic activities of geoconstruction: Areview of recent failure cases", *Arabian J. Geosci.*, **9**(18), 708.

Goh, A.T.C., Zhang, F., Zhang, W.G. and Chew O.Y.S. (2017), "Assessment of strut forces for braced excavation in clays from numerical analysis and field measurements", *Comput. Geotech.*, **86**, 141-149, https://doi.org/10.1016/j.compgeo.2017.01.012.

Han, J. (2014), "Influence of column yielding on degree of consolidation of soft foundations improved by deep mixed columns", *Geomech. Eng.*, **6**(2), 173-194. http://doi-org /10.12989/gae.2014.6.2.173.

Hu, J. and Ma, F. (2018), "Failure investigation at a collapsed deep open cut slope excavation in soft clay", *Geotech. Geol. Eng.*, **36**(1), 665-683. http://doi-org/10.1007/s10706-017-0337-2.

Jiang, S., Du, C. and Sun, L. (2018), "Numerical analysis of sheet pile wall structure considering soil-structure interaction", *Geomech. Eng.*, **16**(3), 309-320. https://doi.org/10.12989/gae.2018.16.3.309.

Kim, S.H., Yom, K.S. and Choi, S.M. (2016), "Stress-transfer in concrete encased and filled tube square columns employed in top-down construction", *Steel Compos. Struct.*, **22**(1), 63-77. http://doi-org/10.12989/SCS.2016.22.1.063.

Kog, Y.C. (2017), "Excavation-induced settlement and tilt of a 3-story building", *J. Perform. Constr. Facil.*, **31**(1), 04016080. https://doi.org/10.1061/(ASCE)CF.1943-5509.0000935.

Li, D., Li, Z. and Tang, D. (2015), "Three-dimensional effects on deformation of deep excavations. Geotechnical Engineering", *Proc. Inst. Civ. Eng. - Geotech. Eng.*, **168**(6), 551-562. https://doi.org/10.1680/jgeen.15.00042.

Lin, L. (2011), "Shrinkage induced tension in reinforced concrete struts for retaining large-scale excavation", *Adv. Mater. Res.*, **368**, 2880-2886. https://doi.org/10.4028/www.scientific.net/AMR.368-373.2880.

Liu, G.B., Jiang, R.J., Ng, C.W.W. and Hong, Y. (2011), "Deformation characteristics of a 38m deep excavation in soft clay", *Can. Geotech. J.*, **48**(12): 1817-1828. https://doi.org/10.1139/t11-075.

Liu, J.G., Zhou, D.D. and Liu, K. (2015), "A mathematical model to recover missing monitoring data of foundation pit", *Geomech. Eng.*, **9**(3), 275-286. https://doi.org/10.12989/gae.2015.9.3.275.

Ng, C.W.W. (1992), "An evaluation of soil-structure interaction associated with a multipropped excavation", Ph.D Dissertation, University of Bristol, Bristol.

Paik, K.H. and Salgado, R. (2003), "Estimation of active earth pressure against rigid retaining walls considering arching effects", *Géotechnique*, **53**(7), 643-653. http://doi-org/10.1680/geot.2003.53.7.643.

Peck, R.B. (1969), "Deep excavation & tunneling in soft ground. Stateof-the-art-report", *Proc., Int. Conf. of Soil Mechanics and Foundation Engineering*, Int. Society for Soil Mechanics and Geotechnical Engineering, London, 225–281.

Tan, Y. and Li, M. (2011), "Measured performance of a 26m deep top-down excavation in downtown Shanghai", *Can Geotech. J.*, **48**(5): 704-719. https://doi.org/10.1139/t10-100.

Ukritchon, B., Faustino, J.C. and Keawsawasvong, S. (2016), "Numerical investigations of pile load distribution in pile group foundation subjected to vertical load and large moment", *Geomech. Eng.*, **10**(5), 577-598. https://doi.org/10.12989/gae.2016.10.5.577.

Wu, M., Du, C.H., Yang, K., Geng, X.Y., Liu, X. and Xia, T.D. (2019), "A new empirical approach to estimate temperature effects on strut loads in braced excavation", *Tunn. Undergr. Sp. Technol.*, **94**, 103-115. https://doi.org/10.1016/j.tust.2019.103115.

Xu, C.J., Ding, H.B., Luo, W.J., Tong, L.H., Chen, Q.S. and Deng, J.L. (2020), "Experimental and numerical study on performance of long-short combined retaining piles", *Geomech. Eng.*, **20**(3), 255-265. http://doi-org/10.12989/gae.2020.20.3.255.

Yang, X.L. (2007), "Upper bound limit analysis of active earth pressure with different fracture surface and nonlinear yield criterion", *Theor. Appl. Fract. Mec.*, **47**(1), 46-56. https://doi.org/10.1016/j.tafmec.2006.10.003.

Zhang, J., Xie, R. and Zhang, H. (2018a), "Mechanical response analysis of the buried pipeline due to adjacent foundation pit excavation", *Tunn. Undergr. Sp. Technol.*, **78**, 135-145. https://doi.org/10.1016/j.tust.2018.04.026.

Zhang, W.G., Goh, A.T.C., Goh, K.H., Chew, O.Y.S., Zhou, D. and Zhang, R. (2018b), "Performance of braced excavation in residual soil with groundwater drawdown", *Undergr. Sp.*, **3**,

150-165. https://doi.org/10.1016/j.undsp.2018.03.002.
Zhang, Z.G., Zhao, Q.H. and Zhang, M.X. (2016), "Deformation analyses during subway shield excavation considering stiffness influences of underground structures", *Geomech. Eng.*, **11**(1), 117–139. http://doi-org/10.12989/gae.2016.11.1.117.
Zheng, G., Du, Y.M., Cheng, X.S., Diao, Y., Deng, X., and Wang, F.J. (2017a), "Characteristics and prediction methods for tunnel deformations induced by excavations", *Geomech. Eng.*, **12**(3), 361-397. https://doi.org/10.12989/gae.2017.12.3.361.
Zheng, G., Zhang, T., Cheng, X.S. and Diao, Y. (2017b), "Statistical analysis of measured data of center post upheaval in metro station excavations in Tianjin", *Rock Soil Mech*., **38**(1), 387-394. In Chinese.

CC